Bottom hypoxia extent off the Changjiang River estuary

Wenxia Zhang, Hui Wu, Zhuoyi Zhu

September 17th, 2018

SKLEC

IMBeR
Integrated Marine Biosphere Research

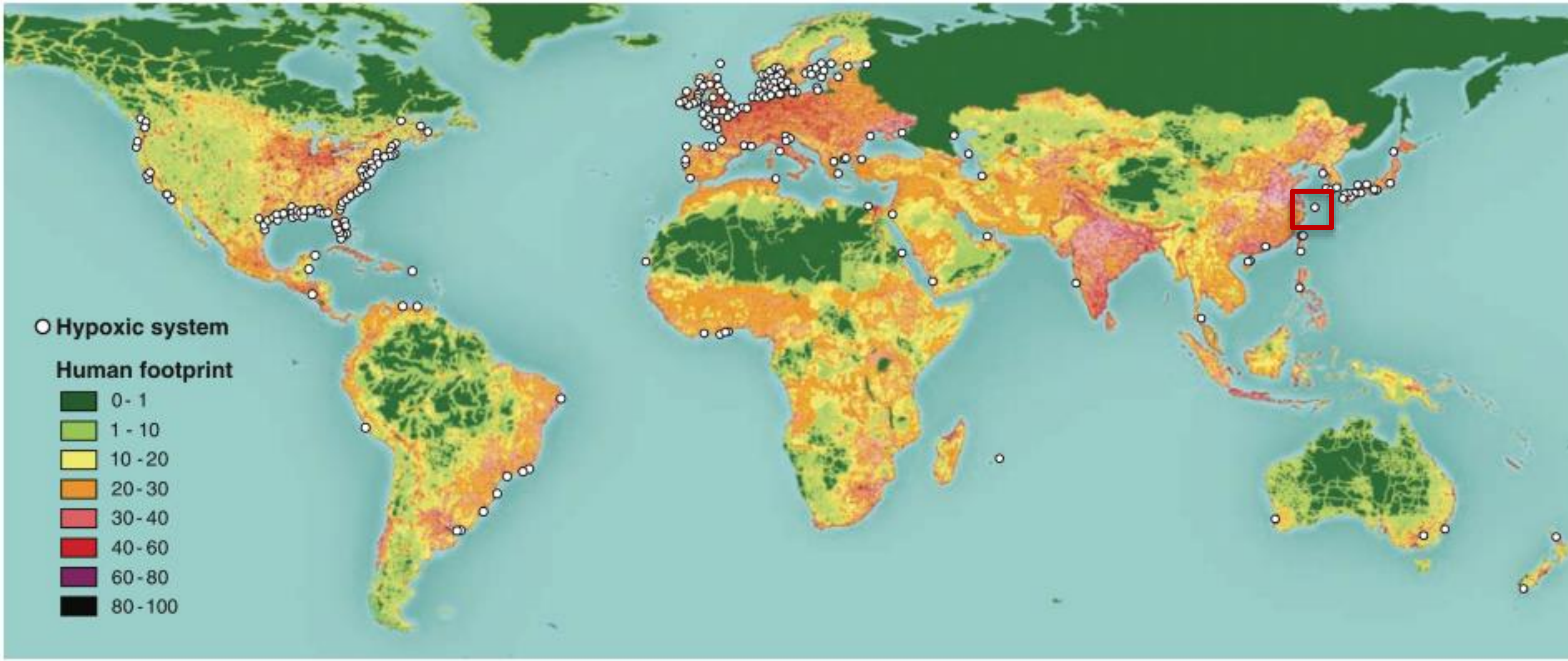

Fig. 1. Global distribution of 400-plus systems that have scientifically reported accounts of being eutrophication-associated dead zones. Their distribution matches the global human footprint [the normalized human influence is expressed as a percent (*41*)] in the Northern Hemisphere. For the Southern Hemisphere, the occurrence of dead zones is only recently being reported. Details on each system are in tables S1 and S2.

Diaz and Rosenberg, 2008

ROMS-based hydrodynamic model

Model setup

30 vertical layers

horizontal resolution is <500 m in the upper estuary, ~1 km in the plume near-field region

Nitrogen, DIP cycle model

nitrate, NO_3; ammonium, NH_4; phosphate, PO_4; phytoplankton; chlorophyll; zooplankton; large detritus, LDet; small detritus, SDet; dissolved oxygen, DO

Air-sea oxygen exchange
Sediment oxygen demand

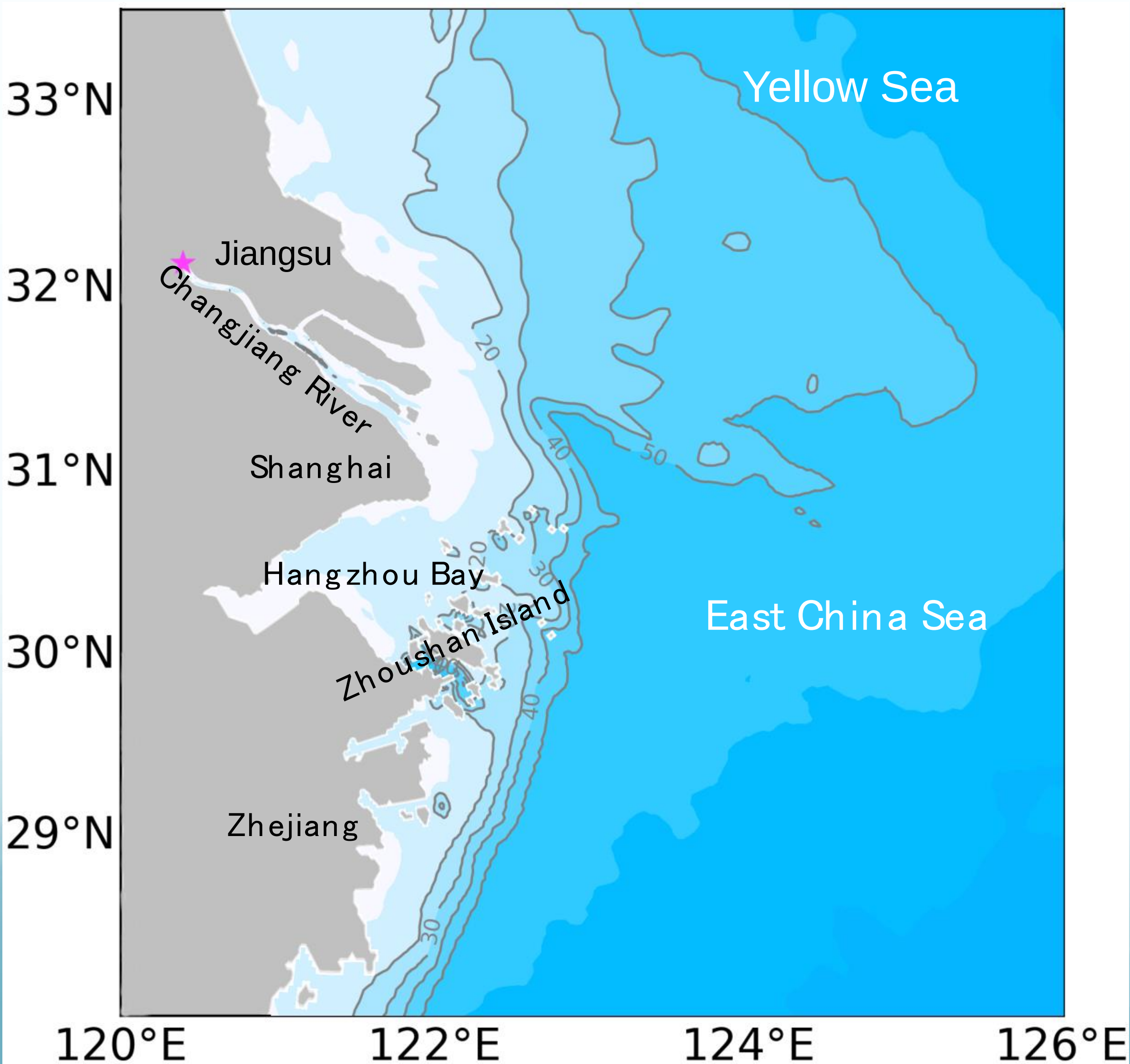

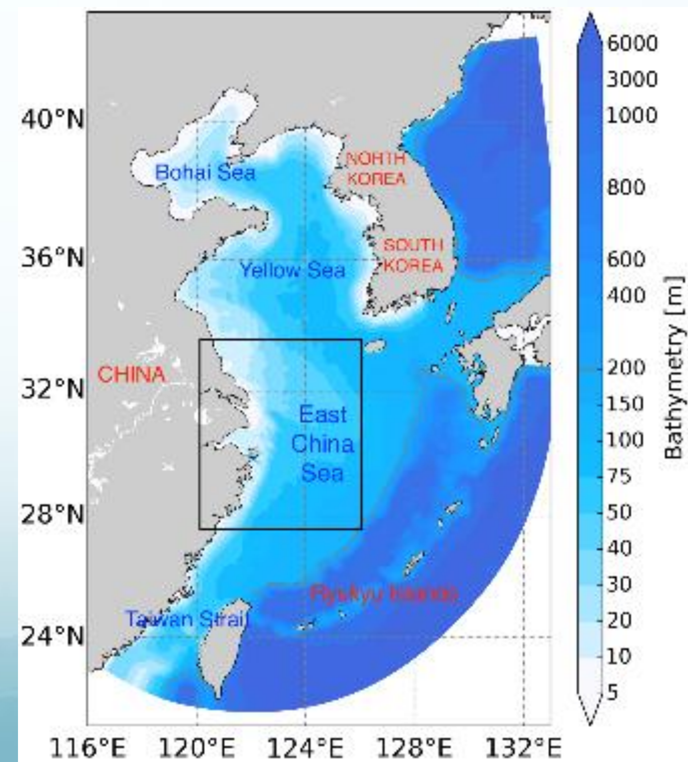

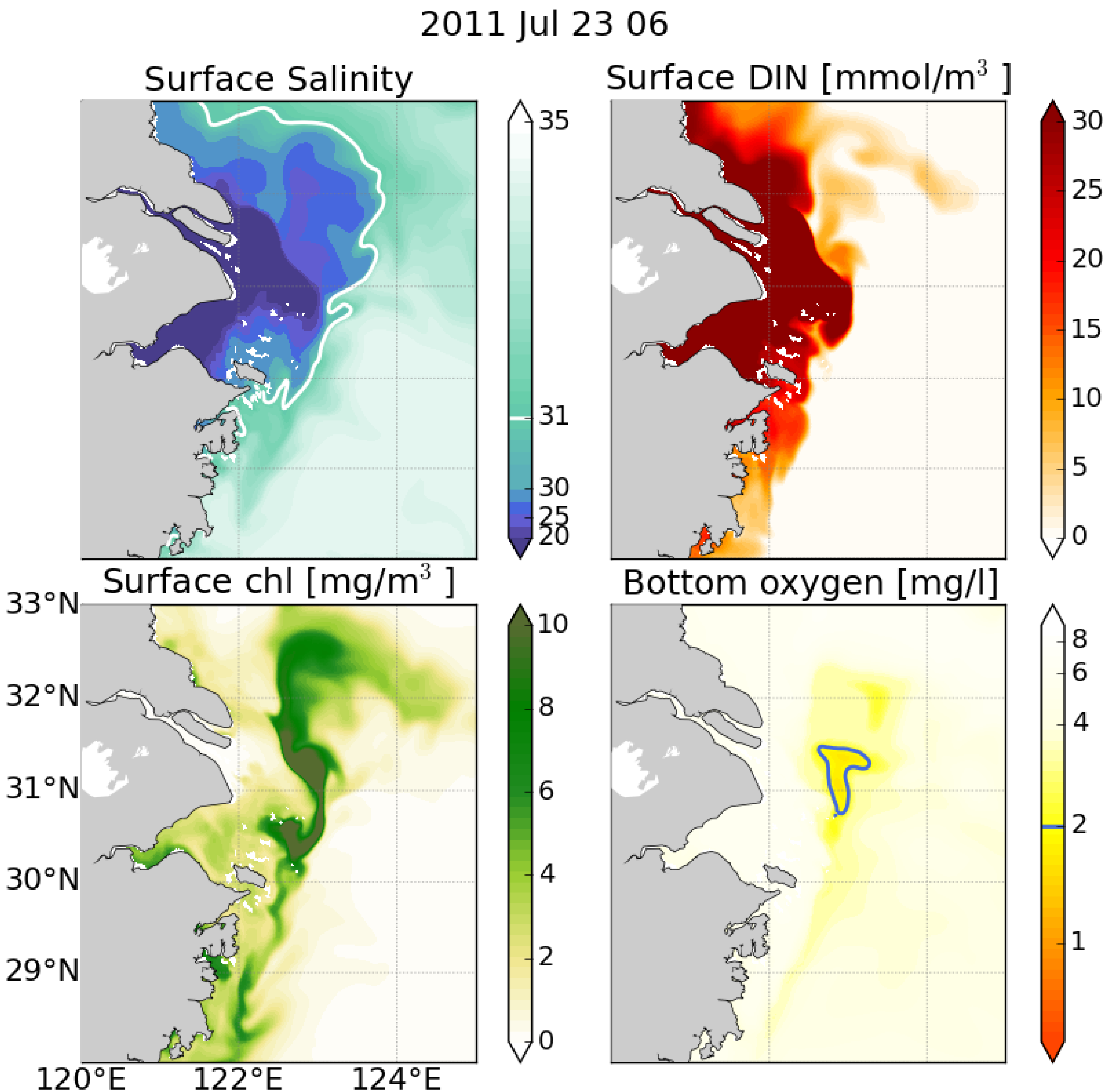
2011 Jul 23 06
Surface Salinity
35
31
30
25
20
Surface DIN [mmol/m3]
30
25
20
15
10
5
0
Surface chl [mg/m3]
10
8
6
4
2
0
Bottom oxygen [mg/l]
8
6
4
2
1
33°N
32°N
31°N
30°N
29°N
120°E
122°E
124°E

Model evaluation

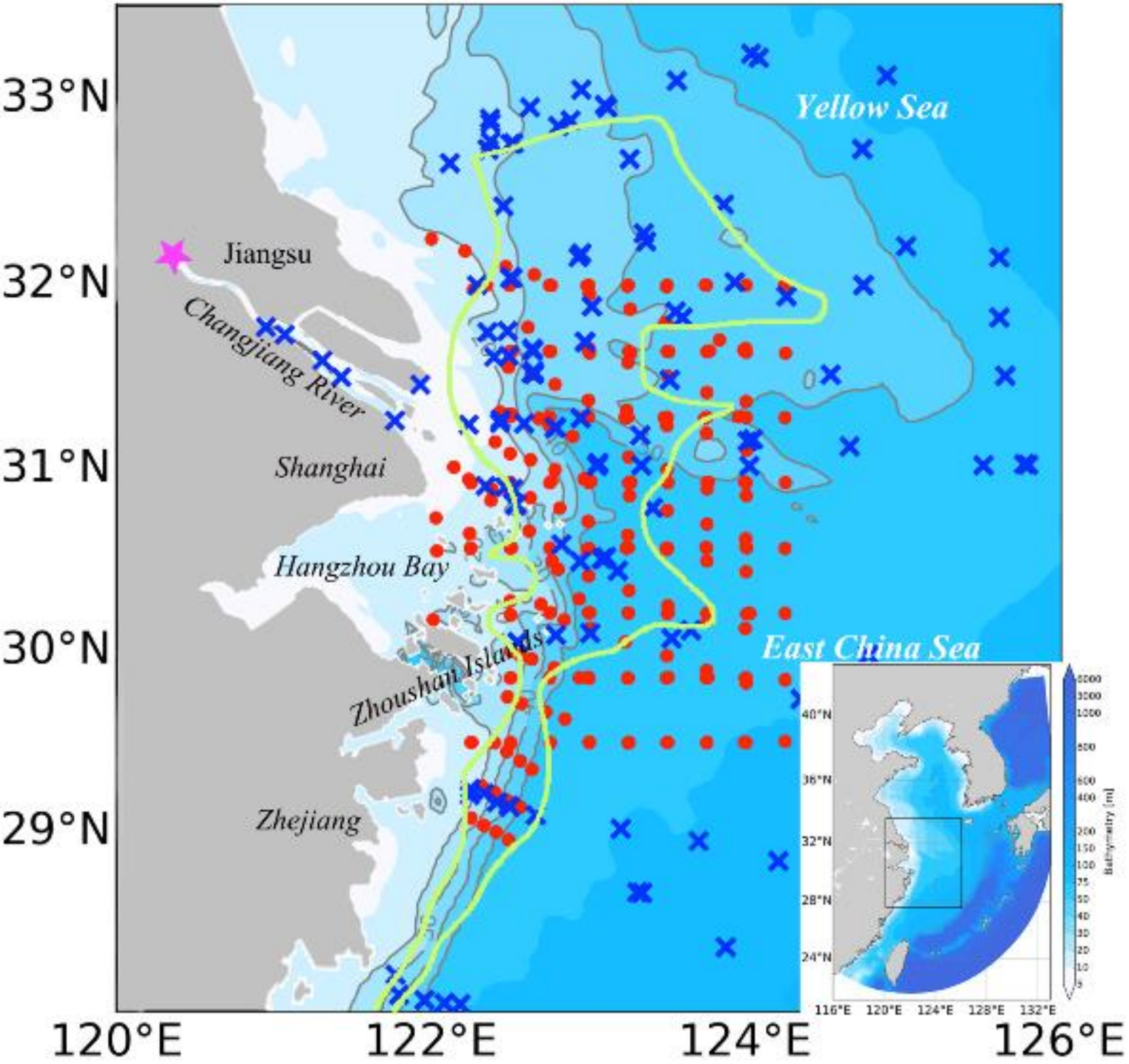

Red point: observed locations for temperature and salinity

Blue cross: observed locations for oxygen concentration

The integrated historical hypoxia extent (marked in cyan) was adopted from Zhou et al., [2017].

Model evaluation

Model-data point-to-point comparisons:

a) Temperature, the solid black line is the linear fit with a slope of 0.92 for all points;
b) salinity, the solid black line is the linear fit with a slope of 1.01 for all points;
c) T-S scatter comparisons, '◦' and '⋆' represent observed and modeled values respectively, orange represents surface values in spring, cyan represents bottom values in spring, red represents surface values in summer, and blue represents bottom values in summer.

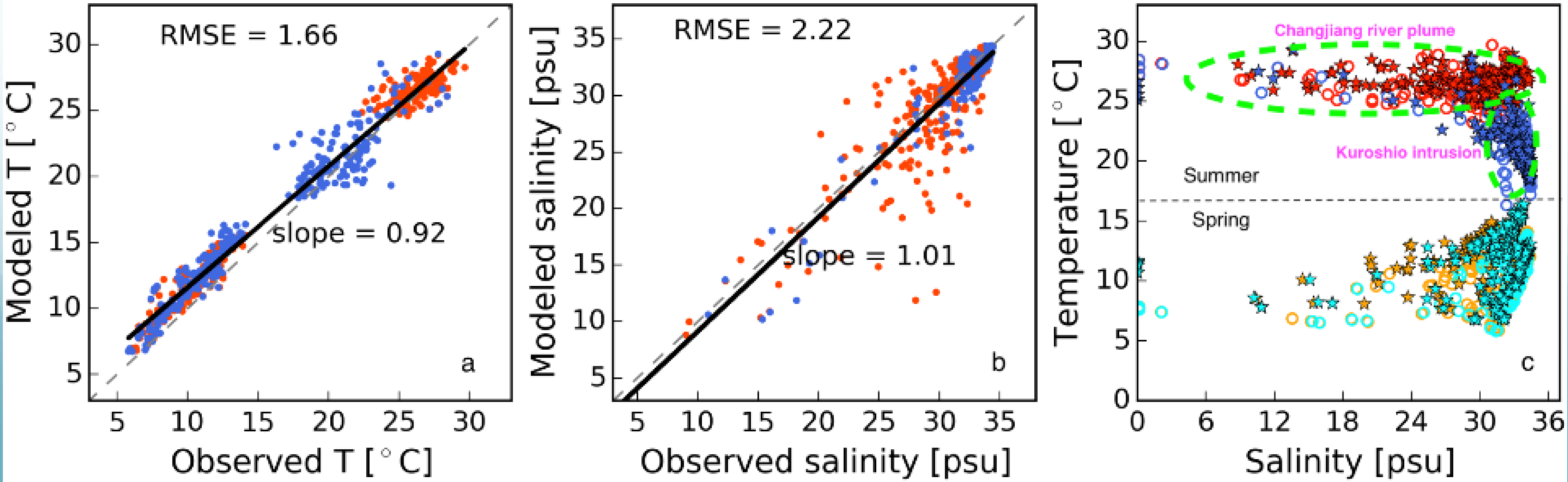

Model evaluation

Model-data point-to-point comparisons:

a) Bottom dissolved oxygen comparison;
b) histogram of observed oxygen concentration minus modeled oxygen concentration;
c) observed BO for one single cruise;
d) modeled BO, observations are superimposed.

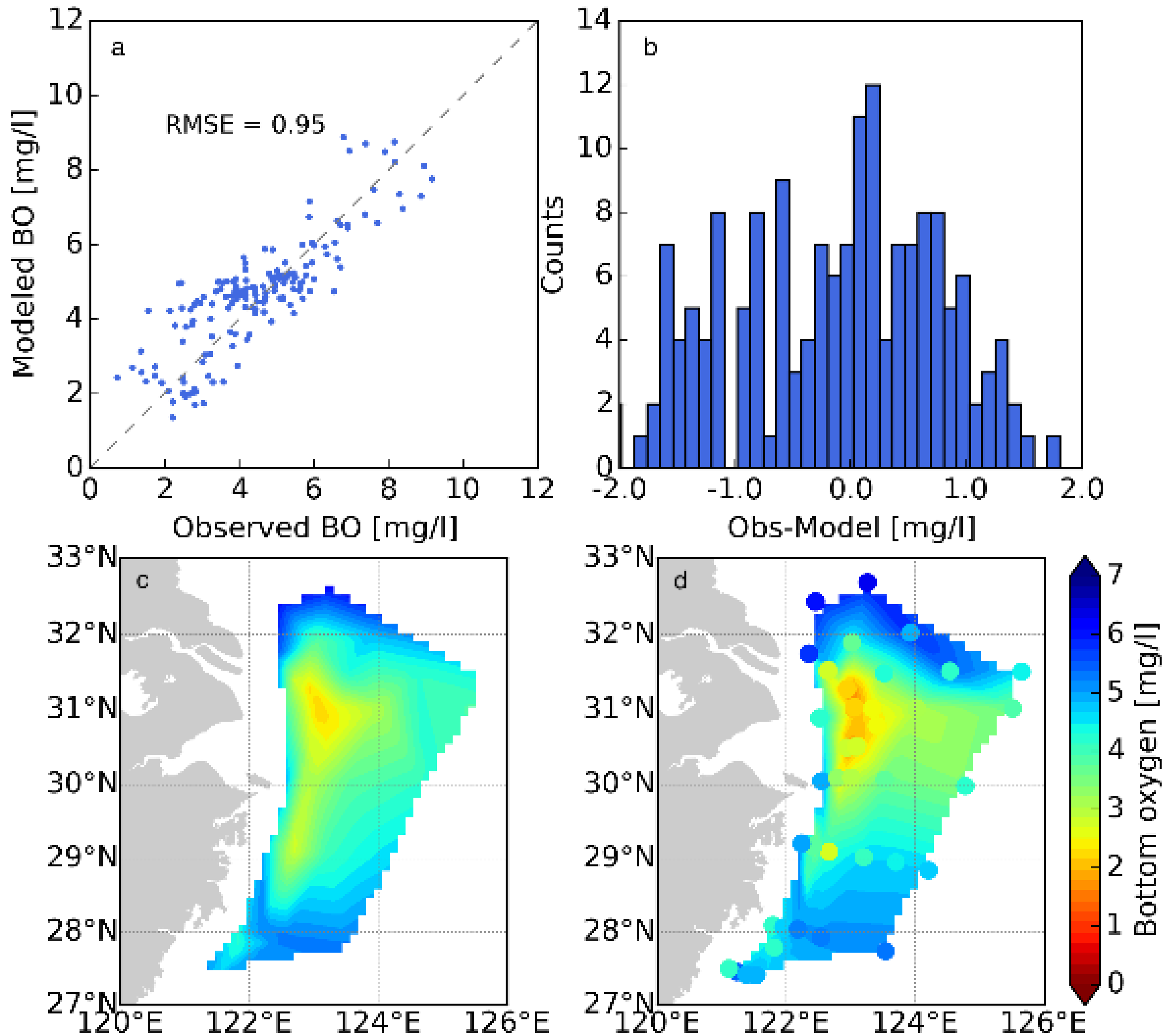

Bottom hypoxia formation and sustain

two stages of calculated vertical stratification maxima and simultaneous bottom oxygen concentration in August 2011

the multi-colored isolines are identical isohaline in panels a,c, and b, d

the superimposed arrows represent simultaneous wind

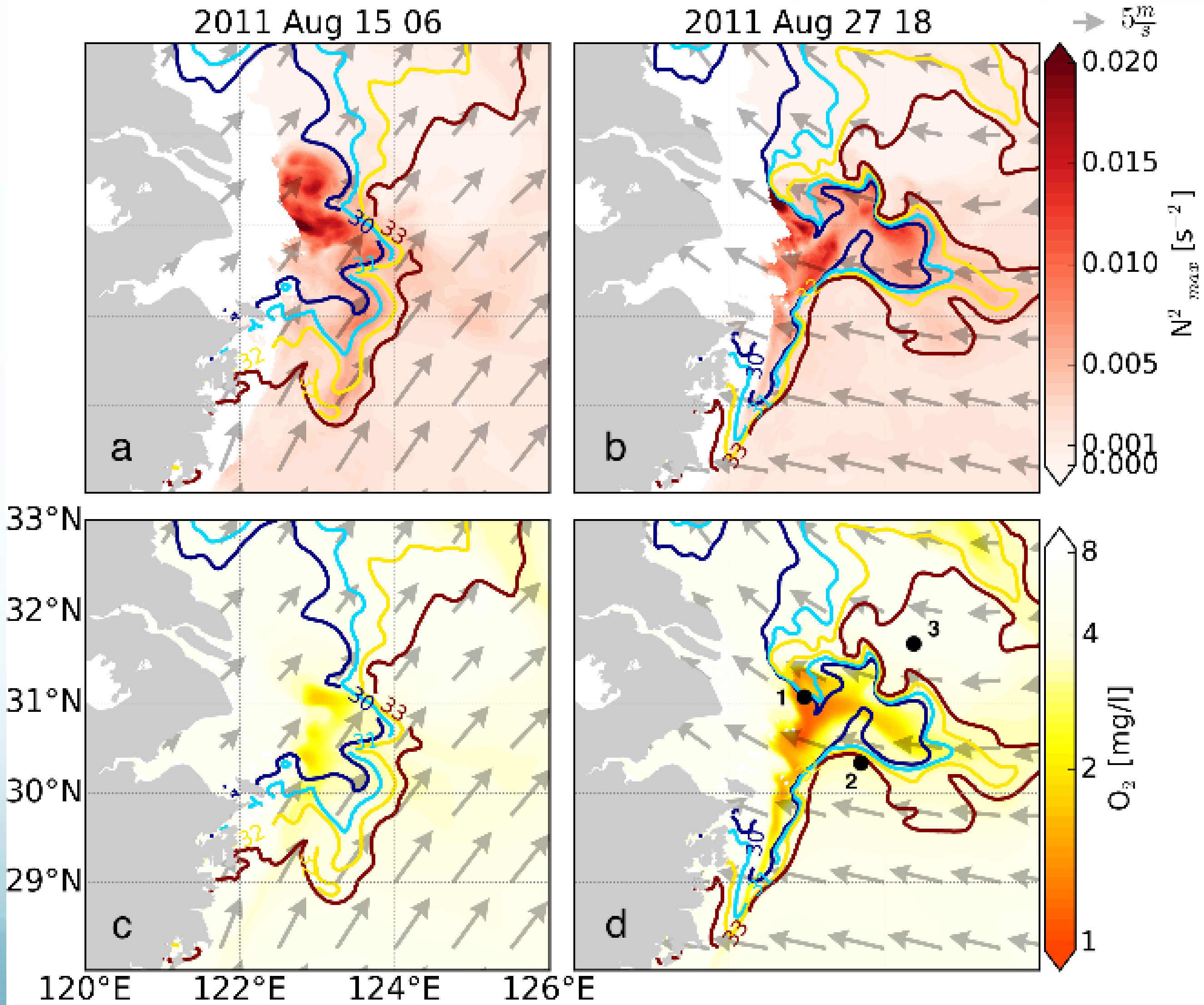

Bottom hypoxia formation and sustain

9 stages of modeled surface salinity evolution in August 2011

simultaneous winds are superimposed

31-psu isohaline is denoted in white

the red contour constrains modeled hypoxic area for each stage

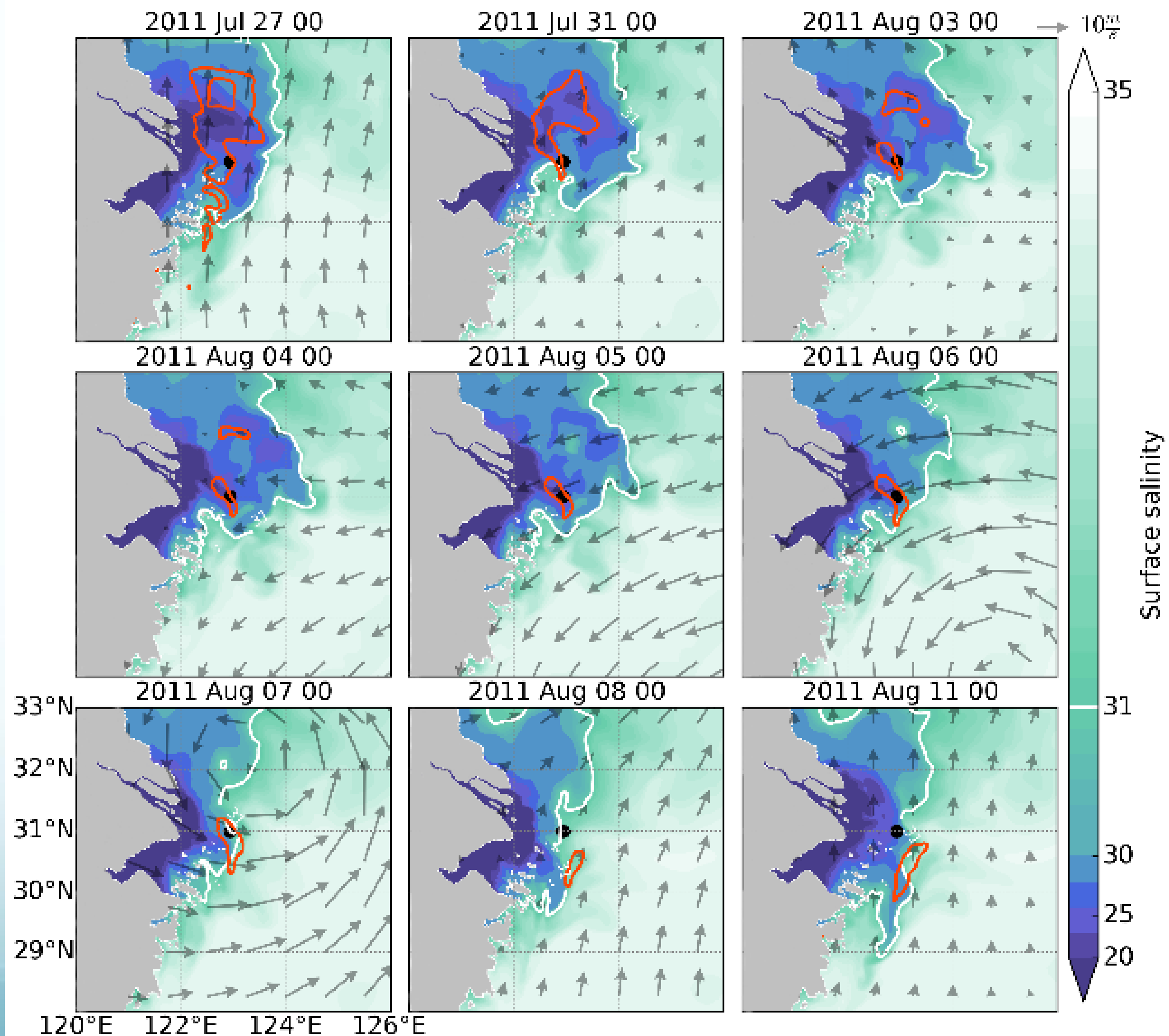

Transient spatial extent of bottom hypoxia

Oxygen budget:

- Advection
- Diffusion
- Water column respiration
- Air-sea flux
- Primary production
- Nitrification
- Sediment oxygen demand

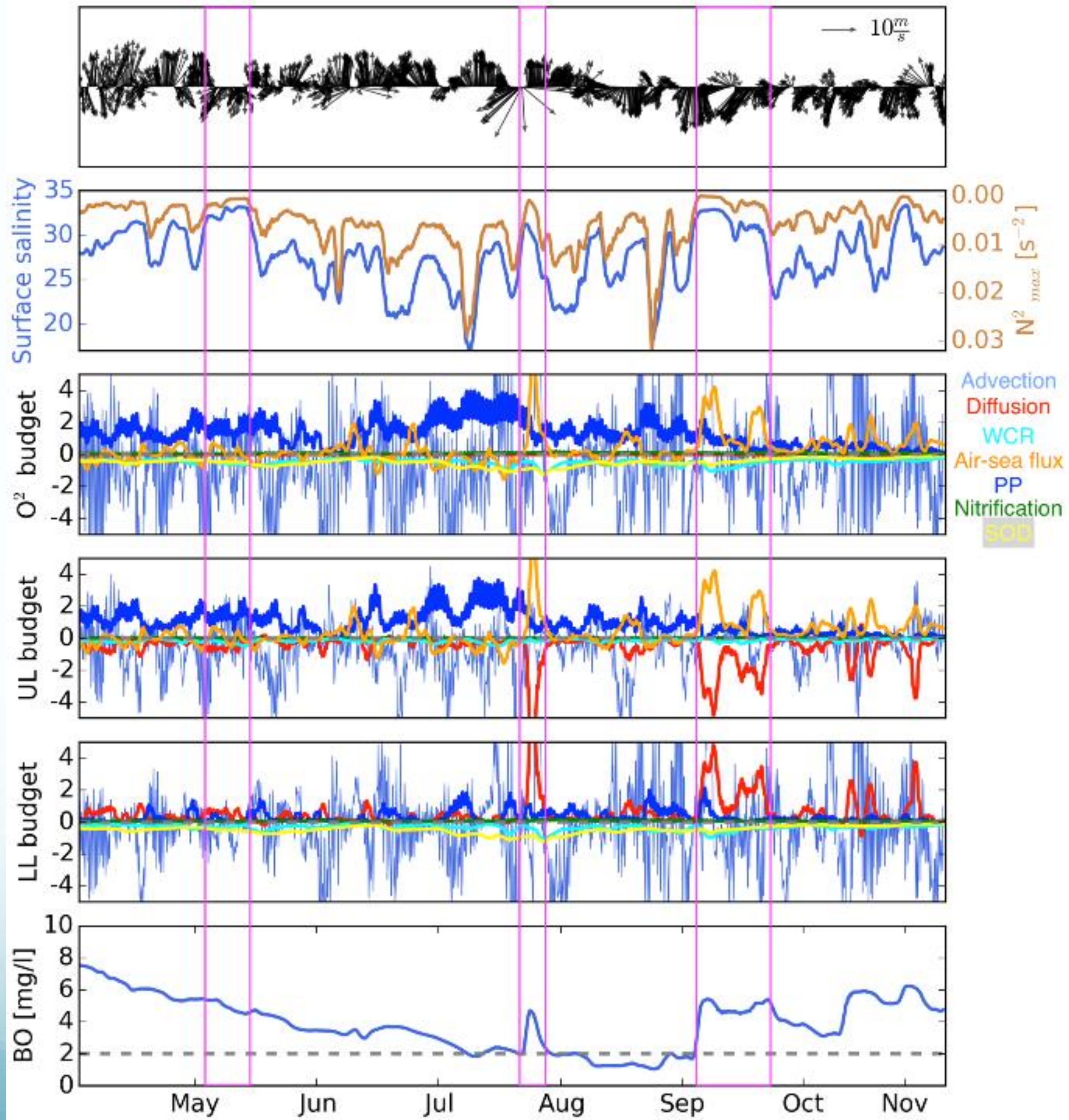

Transient spatial extent of bottom hypoxia

a) Modeled bottom dissolved oxygen corresponding to observation

a) plan-view (3-hourly output averaged to daily) and c) time series (3-hourly) of modeled bottom hypoxic area over the date range of this cruise

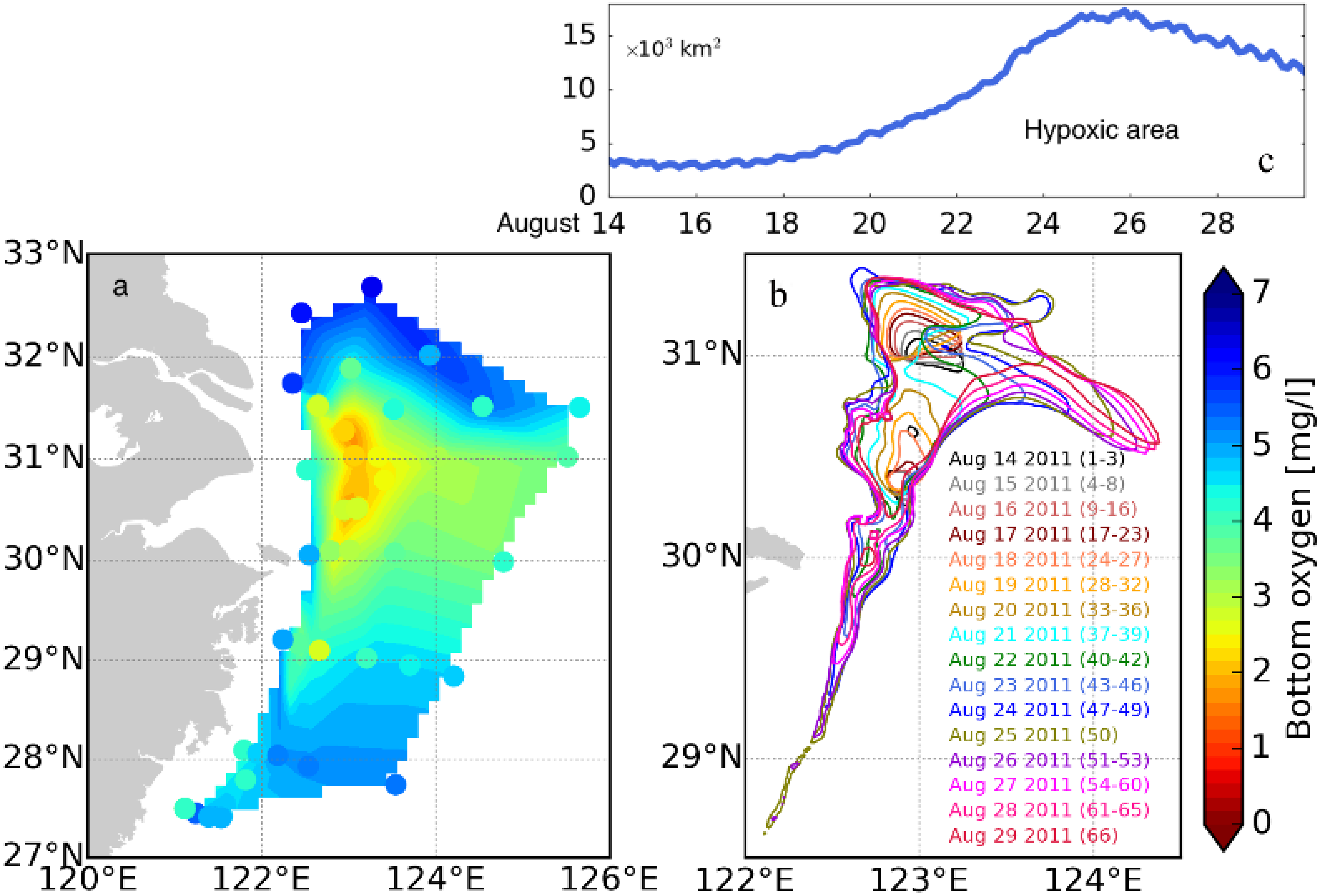

Conclusions

Freshwater shows fast response to wind; subsequent stratification is phase-locked with river plume, which bottom low oxygen generally co-locates;

Short-time bottom oxygen evolution is predominantly vertical processes dependent, and the relevant air-sea oxygen flux approaches bottom via diffusion during mixing event;

Frequent changes in wind direction and magnitude induce transient spatial extent of bottom hypoxia;

Estimated spatial extent of bottom hypoxia during conventional research cruises could be biased.

Thank you!

Wind and tide regulate spatial extent of Changjiang river plume

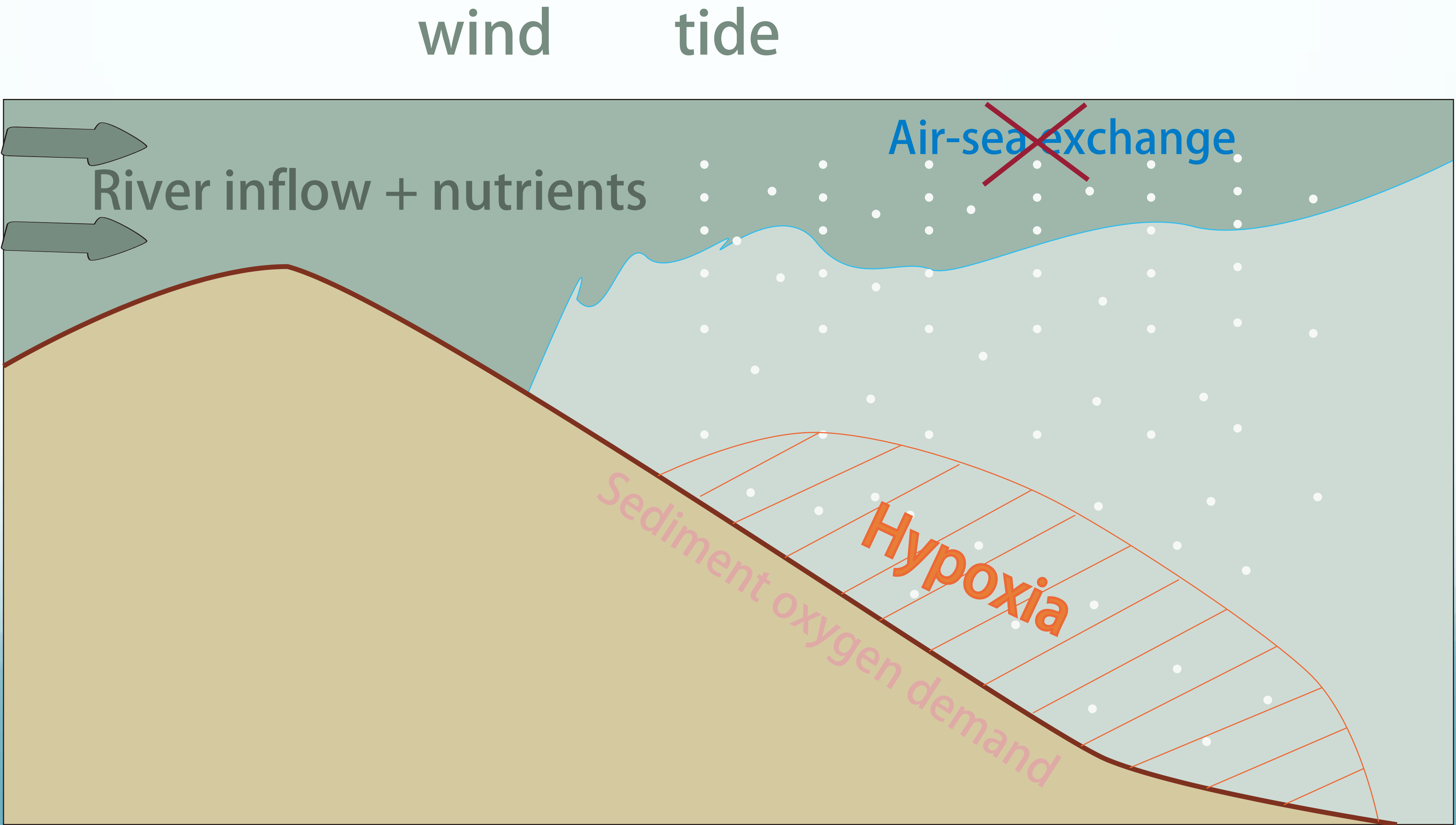

$$\frac{\partial Ox}{\partial t} = -[(u\frac{\partial Ox}{\partial x} + v\frac{\partial Ox}{\partial y} + w\frac{\partial Ox}{\partial z})] + [\frac{\partial}{\partial x}(K_H\frac{\partial Ox}{\partial x}) + \frac{\partial}{\partial y}(K_H\frac{\partial Ox}{\partial y}) + \frac{\partial}{\partial z}(K_V\frac{\partial Ox}{\partial z})] + PP + WCR + Nitrif + F_{SOD} + F_{air-sea}, \quad (1)$$

$$PP = \mu_{max}(T)f(E)(\frac{L_{NO_3^-}}{L_N}R_{O_2:NO_3^-} + \frac{L_{NH_4^+}}{L_N}R_{O_2:NH_4^+})min(L_N, L_P)Phy, \quad (2)$$

$$WCR = -R_{O_2:NH_4^+}(l_{BM}Zoo + l_E\frac{Phy^2}{k_P + Phy^2}\beta Zoo + \hat{r}^N_{SD}SDet + \hat{r}^N_{LD}LDet), \quad (3)$$

$$Nitrif = -\hat{n}NH_4^+, \quad (4)$$

$$SOD = 6.0\left[Ox\ \mathrm{m}^{-2}\mathrm{days}^{-1}\right] \times 2^{T/10.0^\circ\mathrm{C}} \times \left[1 - \exp(-\frac{Ox}{30.0\mu\mathrm{M}\ Ox})\right]; \quad (6)$$

$$F_{air-sea} = \frac{\nu\kappa_{O_2}}{\Delta z}(Ox_{sat} - Ox), \quad (7)$$

Parameter	Value	Parameter Description	Units
μ_0	0.59	Phytoplankton growth rate at 0°C	day^{-1}
α	0.025	Initial slope of the instantaneous growth rate vs light curve	$(\text{W m}^{-2})^{-1}\text{day}^{-1}$
k_P	2	Phytoplankton ingestion half saturation concentration	$(\text{mmol N m}^{-3})^2$
$\hat{n}$	0.2	Nitrification rate	day^{-1}
β	0.75	Assimilation efficiency	Dimensionless
l_{BM}	0.1	Excretion rate due to basal metabolism	day^{-1}
l_E	0.1	Maximum rate of assimilation related excretion	day^{-1}
$\hat{r}_{SD}^{N}$	0.3	Remineralization rate of suspended detritus N	day^{-1}
$\hat{r}_{LD}^{N}$	0.01	Remineralization rate of large detritus N	day^{-1}
$R_{O_2:NO_3^-}$	8.625	O_2 produced per mol of NO_3^- assimilated during photosynthesis	$\text{mmol } O_2(\text{mmol } NO_3^-)^{-1}$
$R_{O_2:NH_4^+}$	6.625	O_2 produced per mol of NH_4^+ assimilated during photosynthesis	$\text{mmol } O_2(\text{mmol } NH_4^+)^{-1}$
$AttSW$	0.08	Light attenuation due to seawater	m^{-1}
$AttChl$	0.06	Light attenuation due to chlorophyll	$(\text{mg Chl m}^{-2})^{-1}$
$AttSed$	model description	Light attenuation due to sediment	m^{-1}